*International Journal of Advanced Geosciences*, 14 (1) (2026) 30-36

International Journal of Advanced Geosciences

*Website: www.sciencepubco.com/index.php/IJAG*
*https://doi.org/10.14419/m1y49p48*
***Research paper***

# Determination of Geoidal Undulation of Points Within the Federal University of Technology, Akure, Using Geometric Technique

**Gafar Suara *, Aminat O. Akinola, Adeola O. Tifase, Abdqudus A. Odeyinka**

*Department of Surveying and Geoinformatics, Federal University of Technology, PMB 704, Akure, Ondo State, Nigeria*
**Corresponding author E-mail: gsuara@futa.edu.ng*

*Received: February 10, 2026, Accepted: March 10, 2026, Published: March 14, 2026*

**Abstract**

This study determined the local geoidal undulation at thirty-one (31) points within the Federal University of Technology, Akure, using a geometric method. Before data collection, a two-peg test was performed on the Leica automatic level, resulting in a misclosure of 0.002 m, which verified the instrument's suitability for precise levelling. Similarly, the Differential Global Positioning System (DGPS) receiver was checked for optimal performance. Orthometric heights were obtained through geodetic levelling observations using the height-of-instrument method, while ellipsoidal heights were measured with a Tersus DGPS receiver and processed with Geomatics Office software. Geoidal undulations were calculated as the difference between the ellipsoidal and orthometric heights. The resulting values were used to generate geoidal contour maps and a three-dimensional surface model in Surfer 11 software, enabling visualization of the spatial variation and slope characteristics of the study area. Validation of the results against previously established gravimetric geoidal undulations showed good agreement, with standard deviations and RMSE of 0.234 mm and 0.231 mm, respectively, demonstrating the reliability and accuracy of the geometric method for local geoid determination. As demonstrated in this study, the geometric technique's efficiency, low operational cost, and minimal data requirements make it a viable alternative for determining geoidal undulation in regions with similar terrain, particularly where gravimetric data are unavailable or financially restrictive.

***Keywords***: *DGPS; Geoidal Undulation; Geometric Technique; Gravimetric Data; Levelling.*

## 1. Introduction

Determining the geoid is a fundamental objective in geodesy, as it establishes the reference surface for conventional heights above mean sea level (Jekeli & Kwon, 2002). The geoid is the equipotential surface of Earth's gravity field, which is perpendicular to the direction of gravity at observation points and provides the most accurate estimate of undisturbed mean sea level beneath the continents. Despite its global undulations, the geoid surface is much smoother than Earth's natural surface (Aleem et al., 2016). Consequently, finding the geoid involves assessing the geoidal undulation (N) from a reference ellipsoid. This undulation shows its relationship with topography and the Earth's internal dynamic structure. Understanding the geoid is generally essential for practical tasks such as surveying, cartography, navigation, orbit determination for artificial satellites, and geophysical research of the Earth's crust. A local geoid model is crucial for a country's development (Odera et al., 2014). With the advancement of Global Positioning Systems (GPS), orthometric height can be measured easily when a geoid model is available (Arisauna et al., 2015). Geoid undulation is defined as the distance between the reference ellipsoid and the geoid surface measured along the normal to the ellipsoid. The calculation of geoidal undulation at each point can be performed using the formula:

$$N = h - H$$

The geoidal height is the difference between the reference ellipsoid and the geoid at a specific point. Accurate geoid heights are vital for converting ellipsoidal heights into orthometric heights. Recent advancements in local geoid modelling have incorporated GNSS/levelling data with gravimetric information and enhanced adjustment techniques, achieving centimetre-level accuracy in regions such as Indonesia and Lebanon. These studies also reveal systematic differences from global models, highlighting the need for localised solutions (Mustafin & Moussa, 2024; Prijatna et al., 2024). Moreover, satellite gravity missions like GRACE and GOCE supply essential long-wavelength gravity data that improve regional models and link them to the global geopotential, thereby boosting height conversions. Widely used global geoid models, such as EGM2008 and EGM2020, integrate satellite, terrestrial, airborne, and altimetric data to produce detailed global fields. However, regional discrepancies with GNSS/levelling benchmarks emphasise the importance of considering local solutions, such as campus- or city-scale models, as enhancements to the global framework (Barnes et al., 2019; UN-GGCE). This study aims to

**Copyright © Gafar Suara et al. This is an open access article distributed under the Creative Commons Attribution License, which permits unrestricted use, distribution, and reproduction in any medium, provided the original work is properly cited.**

determine the geoidal heights of points within the Federal University of Technology, Akure, in Ondo State, Nigeria, using geometric techniques.

### 1.1. Study area

The study area is the Federal University of Technology, Akure, Ondo State, Nigeria. It is located within the Akure South Local Government Area of Ondo State (Babalola et al., 2019). It is a major institution in the state, lying between latitudes 7°18'03"N and 7°18'06"N and longitudes 5°8'02"E and 5°8'05"E, and it is characterised by a gentle slope topography (Akintorinwa & Oluwole, 2018). It covered approximately 300 hectares of land, with an average elevation of 374m.

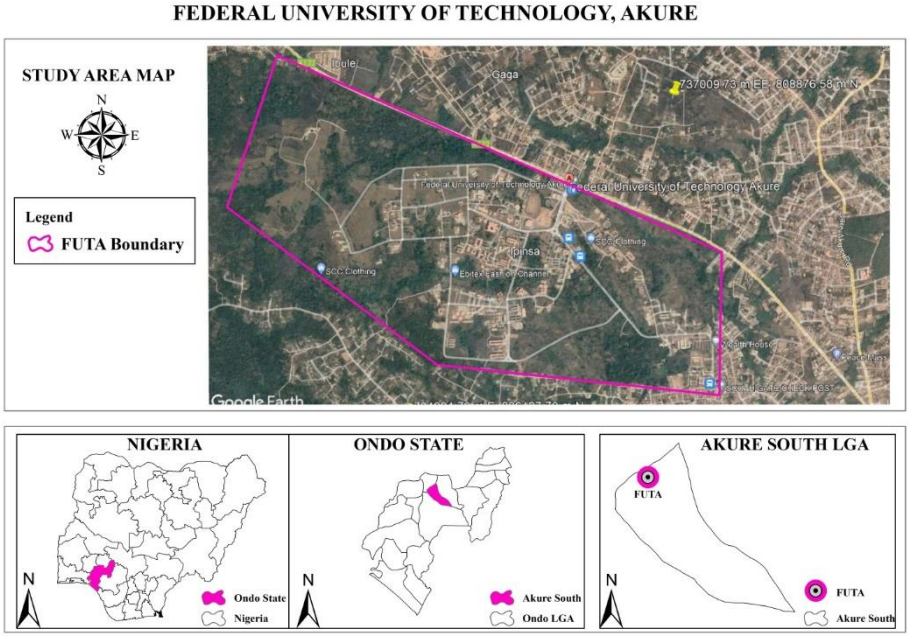



**Fig. 1:** Study Area Map.

## 2. Methodology

This involves the method of data observation, data quality checks, testing, and the processing of the data used in this study.

### 2.1. Data acquisition

The data were mainly collected using Tersus Differential Global Positioning System (DGPS) and Leica Level instruments. The quality was maintained through instrument testing and control beacon checks. Tests were carried out on both the DGPS and the Level instruments. Two peg tests were performed with the Level instrument, achieving an accuracy of 0.002 m (Suara, 2022). Based on the testing results, both instruments were in good working condition for data collection, and the control points remained in position. The data include orthometric heights from geodetic levelling and ellipsoidal heights from differential GPS observations. A total of thirty-one (31) stations, comprising existing beacons, were used. The geodetic coordinates (φ, λ, h) of the points were obtained in static mode. The observation method involved post-processing, with the base receiver positioned at the control station and the rover receiver moved between pillars to capture all selected points. For each control point, DGPS observations were collected for nearly one hour to ensure adequate satellite geometry and reduce positioning errors. The Position Dilution of Precision (PDOP) value during GPS observation remained below 4.0 throughout. The baseline lengths were maintained within optimal limits for static DGPS surveys, with the distance between stations carefully controlled to preserve high-precision phase measurements. A Leica level instrument was used to acquire levelling data using a closed-loop method to minimise errors and ensure accuracy.

### 2.2. Data quality

The quality of data used in any observation depends on its precision and accuracy. Precision relates to validity, while accuracy pertains to reliability (Suara & Idowu, 2019; Idowu et al., 2009). After data collection, a levelling check, also called an arithmetic check, was performed on all levelling readings to verify their accuracy. The differences between the total backsight readings and the total foresight readings, as well as between the initial and final reduced levels, were compared to assess the accuracy of the values and calculations. The results in Table 1 indicate that the geodetic levelling observations were accurately performed, i.e., Last

R.L – first R.L (1)

Where B.S = Back Sight reading, F.S = Fore Sight reading, R.L = Reduced Level.

### 2.3. Data processing

Data processing involves steps such as extracting raw data from DGPS receivers for the benchmarks by connecting them to the computer system (Adeseye & Suara, 2021; Suara & Idowu, 2026). Tersus Geomatics' office solution was used to process raw data, producing adjusted

coordinates and ellipsoidal heights. The processing in the Geomatics software adhered to recommended geodetic standards, incorporating atmospheric models, baseline-adjustment settings, ambiguity-resolution procedures, and quality-control thresholds to ensure accuracy and consistency. The height of instrument (H.I.) method was employed to compute and reduce levelling data and determine the reduced level of each station. This process was simplified by developing an MS Excel programme for the reduction. The height of the control, used as a benchmark, was added to the backsight (B.S.) to determine the instrument's height, as shown in (2).

$$B.S + R.L = H.I \tag{2}$$

The intermediate sight (I.S) and foresight (F.S) at each station were deducted from the height of the instrument to determine the reduced level of each station, as shown in (3).

$$R.L = H.I - F.S/I.S \tag{3}$$

Correction was then made to each station by subtracting the first reduced level from the last reduced level; the value obtained was then distributed along each station using (4).

$$\left(\frac{\text{error}}{\text{total number of stations}}\right) \times \text{each station} \tag{4}$$

The result of the data processing is shown in Table 1.

**Table 1:** Sample Levelling Field Data Processing and Reduction

| Station from | B.S | I.S | F.S | H.I | R.L | Correction | Corrected R.L | Station to |
|---|---|---|---|---|---|---|---|---|
| | 0.923 | | | 353.559 | 352.636 | | | SVG/G15/21 |
| SVG/G15/21 | 2.54 | | 2.62 | 353.479 | 350.939 | -0.0085 | 350.9305 | SVG/G15/20 |
| SVG/G15/20 | | | 0.86 | | 352.619 | -0.0085 | 352.6105 | SVG/G15/21 |
| ACCURACY CHECK | 3.463 | -0.017 | 3.48 | | -0.017 | | | |
| | 3.94 | | | 354.8705 | 350.9305 | | | SVG/G15/20 |
| SVG/G15/20 | 0.61 | | 0.672 | 354.8085 | 354.1985 | -0.001 | 354.1975 | CP1 |
| CP1 | | | 3.88 | | 350.9285 | -0.001 | 350.9275 | SVG/G15/20 |
| ACCURACY CHECK | 4.55 | -0.002 | 4.552 | | -0.002 | | | |
| | 3.413 | | | 357.6105 | 354.1975 | | | CP1 |
| CP1 | 0.279 | | 0.304 | 357.5855 | 357.3065 | 0.0025 | 357.309 | CP2 |
| CP2 | | | 3.383 | | 354.2025 | 0.0025 | 354.205 | CP1 |
| ACCURACY CHECK | 3.692 | 0.005 | 3.687 | | 0.005 | | | |
| | 2.47 | | | 359.779 | 357.309 | | | CP2 |
| CP2 | 0.291 | | 0.32 | 359.75 | 359.459 | -0.0065 | 359.4525 | CP3 |
| CP3 | | | 2.454 | | 357.296 | -0.0065 | 357.2895 | CP2 |
| ACCURACY CHECK | 2.761 | -0.013 | 2.774 | | -0.013 | | | |
| | 2.433 | | | 361.8855 | 359.4525 | | | CP3 |
| CP3 | 0.311 | | 0.332 | 361.8645 | 361.5535 | 0.0005 | 361.554 | CP4 |
| CP4 | | | 2.411 | | 359.4535 | 0.0005 | 359.454 | CP3 |
| ACCURACY CHECK | 2.744 | 0.001 | 2.743 | | 0.001 | | | |
| | 3.02 | | | 364.574 | 361.554 | | | CP4 |
| CP4 | 0.123 | | 0.022 | 364.675 | 364.552 | -0.0195 | 364.5325 | SVG/G15/19 |
| SVG/G15/19 | | | 3.16 | | 361.515 | -0.0195 | 361.4955 | CP4 |
| ACCURACY CHECK | 3.143 | -0.039 | 3.182 | | -0.039 | | | |
| | 0.85 | | | 365.3825 | 364.5325 | | | SVG/G15/19 |
| SVG/G15/19 | 2.21 | | 2.188 | 365.4045 | 363.1945 | 0.001 | 363.1955 | CP5 |
| CP5 | | | 0.87 | | 364.5345 | 0.001 | 364.5355 | SVG/G15/19 |
| ACCURACY CHECK | 3.06 | 0.002 | 3.058 | | 0.002 | | | |
| | 0.282 | | | 363.4775 | 363.1955 | | | CP5 |
| CP5 | 0.2 | | 0.181 | 363.4965 | 363.2965 | 0.0005 | 363.297 | SVG/G15/18 |
| SVG/G15/18 | | | 0.3 | | 363.1965 | 0.0005 | 363.197 | CP5 |
| ACCURACY CHECK | 0.482 | 0.001 | 0.481 | | 0.001 | | | |
| | 0.2 | | | 363.497 | 363.297 | | | SVG/G15/18 |
| SVG/G15/18 | 2.91 | | 2.89 | 363.517 | 360.607 | 0.004 | 360.611 | CP6 |
| CP6 | | | 0.212 | | 363.305 | 0.004 | 363.309 | SVG/G15/18 |
| ACCURACY CHECK | 3.11 | 0.008 | 3.102 | | 0.008 | | | |
| | 0.221 | | | 360.832 | 360.611 | | | CP6 |
| CP6 | 3.38 | | 3.471 | 360.741 | 357.361 | 0 | 357.361 | CP7 |
| CP7 | | | 0.13 | | 360.611 | 0 | 360.611 | CP6 |
| ACCURACY CHECK | 3.601 | 0 | 3.601 | | 0 | | | |
| | 0.254 | | | 357.615 | 357.361 | | | CP7 |
| CP7 | 2.784 | | 2.782 | 357.617 | 354.833 | -0.003 | 354.83 | CP8 |
| CP8 | | | 0.262 | | 357.355 | -0.003 | 357.352 | CP7 |
| ACCURACY CHECK | 3.038 | -0.006 | 3.044 | | -0.006 | | | |
| | 0.23 | | | 355.06 | 354.83 | | | CP8 |

| | | | | | | | | |
|---|---|---|---|---|---|---|---|---|
| CP8 | 3.49 | | 3.5 | 355.05 | 351.56 | -0.015 | 351.545 | CP9 |
| CP9 | | | 0.25 | | 354.8 | -0.015 | 354.785 | CP8 |
| ACCURACY CHECK | 3.72 | -0.03 | 3.75 | | -0.03 | | | |
| | 0.17 | | | 351.715 | 351.545 | | | CP9 |
| CP9 | 2.95 | | 2.942 | 351.723 | 348.773 | -0.002 | 348.771 | CP10 |
| CP10 | | | 0.182 | | 351.541 | -0.002 | 351.539 | CP9 |
| ACCURACY CHECK | 3.12 | -0.004 | 3.124 | | -0.004 | | | |

Where CP is the Change Point,

### 2.4. Determination of geoidal undulation

The geoidal undulation of the study area was determined using the relationship between ellipsoidal heights obtained from GPS measurements and orthometric heights obtained from levelling. i.e.

$$N = h - H, \quad (4)$$

Where N is the geoidal undulation in meters,
h is the height obtained from DGPS observation, known as ellipsoidal height in meters.
H is the orthometric height in meters, which was obtained from the adjusted reduced level from levelling computation contained in Table 1. The final computation of the geoidal heights is shown in Table 2.

## 3. Results and Analysis

The results of the geoidal undulations obtained using the geometric observation approach, after processing, are shown and analysed. Table 2 shows the geoidal undulation obtained from the ellipsoidal and orthometric heights.

**Table 2:** Geoidal Undulations Computation from the Geometric Approach

| Station | Ellipsoidal Height (m) | Orthometric Height (m) | Geoidal Undulation (m) |
|---|---|---|---|
| GPS01 | 372.252 | 349.6172 | 22.6350 |
| GPS02 | 375.108 | 352.0397 | 23.0683 |
| SVG/G13/01 | 376.0146 | 352.9447 | 23.0699 |
| SVG/G13/05 | 378.9688 | 348.9077 | 30.0611 |
| SVG/G13/06 | 385.3785 | 355.3092 | 30.0693 |
| SVG/G13/07 | 392.1631 | 364.4332 | 27.7299 |
| SVG/G13/08 | 388.0933 | 360.4232 | 27.6701 |
| SVG/G13/09 | 384.5235 | 356.8132 | 27.7103 |
| SVG/G13/10 | 375.2656 | 352.2282 | 23.0374 |
| SVG/G14/12 | 374.0495 | 343.9957 | 30.0538 |
| SVG/G14/17 | 387.6995 | 357.6392 | 30.0603 |
| SVG/G14/41 | 371.8143 | 341.7582 | 30.0561 |
| SVG/G14/42 | 371.9662 | 342.3142 | 29.6520 |
| SVG/G14/43 | 370.4488 | 340.4032 | 30.0456 |
| SVG/G14/46 | 372.2363 | 342.5462 | 29.6901 |
| SVG/G14/54 | 360.4436 | 338.1922 | 22.2514 |
| SVG/G15/20 | 380.9679 | 350.9305 | 30.0374 |
| SVG/G15/21 | 382.6659 | 352.636 | 30.0299 |
| SVG/G15/22 | 382.7494 | 352.7195 | 30.0299 |
| SVG/G15/23 | 380.9727 | 352.7195 | 28.2532 |
| SVG/G15/24 | 377.8989 | 354.8247 | 23.0742 |
| SVG/G15/25 | 378.7201 | 355.6347 | 23.0854 |
| SVG/G16/28 | 376.5463 | 353.4047 | 23.1416 |
| SVG/G16/29 | 371.5337 | 348.5147 | 23.0190 |
| SVG/G16/30 | 367.6485 | 342.7872 | 24.8613 |
| SVG/G16/31 | 360.731 | 338.4972 | 22.2338 |
| SVG/G16/34 | 359.0978 | 336.8447 | 22.2531 |
| SVG/G16/35 | 362.6858 | 340.4772 | 22.2086 |
| SVG/G16/36 | 362.0111 | 339.7997 | 22.2114 |
| SVG/G16/37 | 360.5849 | 338.4522 | 22.1327 |
| SVG/G16/38 | 359.2321 | 337.0747 | 22.1574 |

Table 3 presents the coordinates and geoidal undulation of points derived from a project conducted at the Federal University of Technology, Akure, in 2019. This geoidal undulation, determined using a gravimetric method, was used to validate the geometric approach results obtained in this study.

**Table 3:** Coordinates of Points and Geoidal Undulations from Gravimetric Approach

| Station | Longitude | Latitude | Geoidal Undulation (m) |
|---|---|---|---|
| GPS01 | 5.1348244 | 7.2985794 | 22.6352 |
| GPS02 | 5.1355899 | 7.2989031 | 23.0684 |
| SVG/G13/01 | 5.1353341 | 7.2984172 | 23.0700 |
| SVG/G13/05 | 5.1328343 | 7.3034195 | 30.0610 |
| SVG/G13/06 | 5.1327751 | 7.3055535 | 30.0695 |
| SVG/G13/07 | 5.1348642 | 7.3044269 | 27.7297 |
| SVG/G13/08 | 5.1358719 | 7.3038691 | 27.6704 |
| SVG/G13/09 | 5.1369805 | 7.3035371 | 27.7101 |

| | | | |
|---|---|---|---|
| SVG/G13/10 | 5.1360098 | 7.3010472 | 23.0376 |
| SVG/G14/12 | 5.1281626 | 7.3032461 | 30.0536 |
| SVG/G14/17 | 5.1328498 | 7.3070134 | 30.0600 |
| SVG/G14/41 | 5.1249278 | 7.3020143 | 30.0563 |
| SVG/G14/42 | 5.1247897 | 7.3023442 | 29.6518 |
| SVG/G14/43 | 5.1239469 | 7.3040427 | 30.0458 |
| SVG/G14/46 | 5.1279322 | 7.3080442 | 29.6903 |
| SVG/G14/54 | 5.1430554 | 7.2983261 | 22.2509 |
| SVG/G15/20 | 5.1395392 | 7.3061071 | 30.0371 |
| SVG/G15/21 | 5.1392418 | 7.3051435 | 30.0301 |
| SVG/G15/22 | 5.1389478 | 7.3038071 | 30.0302 |
| SVG/G15/23 | 5.1397533 | 7.3023134 | 28.2530 |
| SVG/G15/24 | 5.1389950 | 7.3023245 | 23.0745 |
| SVG/G15/25 | 5.1394493 | 7.3012413 | 23.0857 |
| SVG/G16/28 | 5.1401045 | 7.3021915 | 23.1414 |
| SVG/G16/29 | 5.1408935 | 7.3010289 | 23.0188 |
| SVG/G16/30 | 5.1420285 | 7.2998221 | 24.8610 |
| SVG/G16/31 | 5.1429987 | 7.2985263 | 22.2340 |
| SVG/G16/34 | 5.1488283 | 7.2963817 | 22.2529 |
| SVG/G16/35 | 5.1475282 | 7.2964818 | 22.2087 |
| SVG/G16/36 | 5.1495279 | 7.2966049 | 22.2115 |
| SVG/G16/37 | 5.1494825 | 7.2947207 | 22.1329 |
| SVG/G16/38 | 5.1497991 | 7.2930302 | 22.1572 |

Surfer 11 software was employed to develop contour and 3D surface models of the geoidal undulations at 31 points, based on the data in Table 2. The kriging technique was utilised to create a continuous geoid surface by fitting a variogram model to the empirical semi-variance of the observed geoid heights. A spherical variogram model was chosen for its best fit to the empirical variogram, with the associated nugget, sill, and range parameters estimated through iterative fitting and cross-validation (Pebesma & Graeler, 2022; Burrough & McDonell, 2015). The fitted variogram parameters were subsequently employed to interpolate geoidal undulation values across the study area, generating a spatially coherent and optimal 3D surface model (left) and contour plot (right) in Fig. 2. The visualisations of the contour and 3D surface demonstrated that the geoidal heights derived via the geometric technique form an undulating surface.

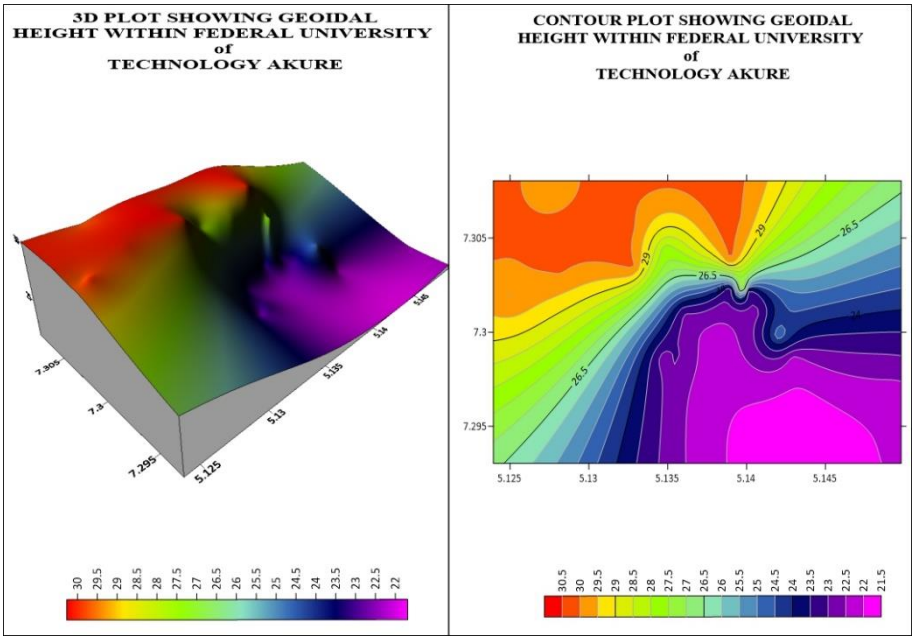



**Fig. 2:** 3D Plot (Left) and Contour Plot (Right) Showing the Geoidal Height Within the Study Area.

Table 4 displays the absolute difference between the geoidal heights determined using the geometric and gravimetric techniques, both observed at the same stations. This is calculated as ΔN = Geometric - Gravimetric.

**Table 4:** Comparison of Gravimetric and Geometric Geoidal Undulations

| Station | Geometric (m) | Gravimetric (m) | Difference ΔN (mm) |
|---|---|---|---|
| GPS01 | 22.6350 | 22.6352 | 0.2 |
| GPS02 | 23.0683 | 23.0684 | 0.1 |
| SVG/G13/01 | 23.0699 | 23.0700 | 0.1 |
| SVG/G13/05 | 30.0611 | 30.0610 | 0.1 |
| SVG/G13/06 | 30.0693 | 30.0695 | 0.2 |
| SVG/G13/07 | 27.7299 | 27.7297 | 0.2 |
| SVG/G13/08 | 27.6701 | 27.6704 | 0.3 |
| SVG/G13/09 | 27.7103 | 27.7101 | 0.2 |
| SVG/G13/10 | 23.0374 | 23.0376 | 0.2 |
| SVG/G14/12 | 30.0538 | 30.0536 | 0.2 |
| SVG/G14/17 | 30.0603 | 30.0600 | 0.3 |
| SVG/G14/41 | 30.0561 | 30.0563 | 0.2 |
| SVG/G14/42 | 29.6520 | 29.6518 | 0.2 |

| | | | |
|---|---|---|---|
| SVG/G14/43 | 30.0456 | 30.0458 | 0.2 |
| SVG/G14/46 | 29.6901 | 29.6903 | 0.2 |
| SVG/G14/54 | 22.2514 | 22.2509 | 0.5 |
| SVG/G15/20 | 30.0374 | 30.0371 | 0.3 |
| SVG/G15/21 | 30.0299 | 30.0301 | 0.2 |
| SVG/G15/22 | 30.0299 | 30.0302 | 0.3 |
| SVG/G15/23 | 28.2532 | 28.2530 | 0.2 |
| SVG/G15/24 | 23.0742 | 23.0745 | 0.3 |
| SVG/G15/25 | 23.0854 | 23.0857 | 0.3 |
| SVG/G16/28 | 23.1416 | 23.1414 | 0.2 |
| SVG/G16/29 | 23.0190 | 23.0188 | 0.2 |
| SVG/G16/30 | 24.8613 | 24.8610 | 0.3 |
| SVG/G16/31 | 22.2338 | 22.2340 | 0.2 |
| SVG/G16/34 | 22.2531 | 22.2529 | 0.2 |
| SVG/G16/35 | 22.2086 | 22.2087 | 0.1 |
| SVG/G16/36 | 22.2114 | 22.2115 | 0.1 |
| SVG/G16/37 | 22.1327 | 22.1329 | 0.2 |
| SVG/G16/38 | 22.1574 | 22.1572 | 0.2 |

The absolute differences for the co-located points in Table 4 show that the variations in geoidal undulations determined by the methods are below 0.5 mm, confirming the reliability of the results obtained through the geometric approach. The accuracy statistics for these results are provided in Table 5.

**Table 5:** Accuracy Statistics

| Metric | Value |
|---|---|
| Mean difference | 0.003 mm |
| Standard deviation | 0.234 mm |
| RMSE | 0.231 mm |
| Mean absolute difference | 0.216 mm |
| Maximum absolute difference | 0.50 mm |

The hypothesis test for the datasets was also conducted at 95% confidence intervals (CI). The test results are displayed in Table 6.

**Table 6:** Student T-Statistic Distribution Test

| Null Hypothesis | Mean (Geometric - Gravimetric) = 0 |
|---|---|
| t-statistic | 0.0766 (df = 30) |
| Two-sided p-value | 0.9395 |
| Conclusion | Accept the null hypothesis, Ho.<br>There is no significant difference between the geometric and gravimetric undulations. |

## 4. Discussion

The comparison between observed geometric and gravimetric geoidal undulations across the 31 stations demonstrates a high level of consistency, with differences in the sub-millimetre range. The mean difference of 0.000003 m (0.003 mm) indicates no systematic deviation between the two types of undulations. This negligible difference is further supported by the paired t-test ($t = 0.0766$, $p = 0.94$), which shows no significant differences between the datasets. The standard deviation of 0.000234 m (about 0.23 mm), along with an RMSE of approximately 0.000231 m, indicates that station-to-station deviations are very small and well within the expected precision of GNSS-based heighting and geoid modelling methods. Spatially, the stations with the largest differences (up to 0.5 mm) do not form any meaningful clusters that might suggest localised distortions in the geoid or systematic GNSS errors. Moreover, the consistency across the geoidal height range of roughly 22 m to 30 m demonstrates that there is no scale-dependent behaviour in the datasets. These results confirm that the geometric geoidal height derived from GNSS/levelling provides a reliable and accurate reference point, meeting the strict standards required for high-quality geodetic control networks, geoscience, and engineering applications that demand reliable and precise height measurements. Still, the determination of geoidal undulation can be influenced by various potential sources of error. GNSS observations may be affected by multipath, where satellite signals reflect off nearby surfaces (e.g., buildings, ground surface) before reaching the antenna, thereby influencing the derived ellipsoidal heights and reducing positioning accuracy, especially in built or reflective environments (Tang et al., 2021). Antenna design, signal processing, and site selection also help mitigate these effects. Levelling misclosures can arise from instrument setup errors, atmospheric refraction, and the gradual accumulation of random errors along the line; forward–backward runs and loop closures are used to detect and control these misclosures in accordance with geodetic-levelling standards. Finally, differences between geoid models may occur between locally determined geometric geoid heights and global or gravimetric models, reflecting variations in the underlying gravity data coverage, modelling techniques, and resolution; such differences are documented regionally and highlight the importance of considering our surface as a local model (Gerlach & Rummel, 2024). It is also important to note that, due to the limited spatial coverage of the 31 observed points, the geoid undulation values derived in this study represent a localised geoid model. Consequently, these results pertain to a local geoid model specific to the study area rather than a regional one.

## 5. Conclusion

This study determined the local geoidal undulations within the Federal University of Technology, Akure, using the geometric method, and subsequently validated the results against previously established gravimetric geoid values for the same area. Ellipsoidal heights were obtained using a Tersus DGPS receiver, while orthometric heights were derived from precise levelling with a Leica instrument. The geometric technique was applied to compute geoidal undulations, followed by a comparative analysis against existing gravimetric geoidal heights. The geometric results showed good agreement with the gravimetric-derived undulations, confirming the reliability and practical accuracy of the geometric approach for local geoid determination. The computed values were further used to generate contour maps and a three-dimensional surface model, providing a clear spatial representation of the geoid across the study area. The validation exercise demonstrates

that the geometric method not only serves as a rapid and cost-effective technique but also produces results consistent with gravimetric solutions when high-quality DGPS and levelling data are available. This positions the geometric approach as a useful alternative for areas where gravimetric data are limited, inaccessible, or prohibitively expensive to obtain. This study establishes that the geometric technique reliably determines local geoidal undulations and can be confidently applied to terrains similar to those of the study area.

## Acknowledgement

We appreciate the support of the Department of Surveying and Geoinformatics at the Federal University of Technology, Akure, in acquiring the data used in this study.

## References

[1] Adeseye, T. A., & Suara, G. (2021). *3D-position determination using GNSS techniques – A comparative analysis*. European Journal of Engineering and Technology Research, *6*(4). https://doi.org/10.24018/ejers.2021.6.4.2435.

[2] Akintorinwa, O. J., & Oluwole, S. T. (2018). Empirical relationship between electrical resistivity and geotechnical parameters: A case study of Federal University of Technology campus, Akure, SW, Nigeria. *NRIAG Journal of Astronomy and Geophysics, 7*(1), 123–133. https://doi.org/10.1016/j.nrjag.2018.02.004.

[3] Aleem, K. F., Adesoye, A. A., & Bankole, A. L. (2016). Practical determination of geoidal undulation and geoidal map of part of Mubi, Adamawa State, Nigeria. *International Journal of Engineering Research and Technology*, *5*(4).

[4] Arisauna, P., Dyah, P., Nabila, S., Adolfientje, K., & Kosasih, P. (2015). *Determination of the gravimetric geoid model in Sulawesi–Indonesia*. FIG Working Week 2015, Sofia, Bulgaria, 17–21 May 2015.

[5] Babalola, S. O., Suara, G., & Oyelakin, L. O. (2019). Spatiotemporal dynamics digital mapping of land use, Obakekere Campus Federal University of Technology, Akure, Nigeria. *European Journal of Advances in Engineering and Technology, 6*(9), 12–19. https://doi.org/10.5281/zenodo.10688613

[6] Barnes, D., Beale, J., Ingalls, S., Small, H., Ganley, R., Minter, C., & Presicci, M. (2019, September 18). *EGM2020: Updates* (Workshop slides). https://www.sirgas.org/fileadmin/docs/GGRF_Wksp/23_Barnes_et_al_2019_EGM2020_Updates.pdf.

[7] Burrough, P. A., & McDonnell, R. A. (2015). *Kriging interpolation*. In *Geospatial Analysis Online*. Retrieved from https://www.spatialanalysisonline.com/HTML/kriging_interpolation.htm.

[8] Gerlach, C., & Rummel, R. (2024). Benefit of classical leveling for geoid-based vertical reference frames. *Journal of Geodesy, 98*, Article 64. https://doi.org/10.1007/s00190-024-01849-y.

[9] Idowu, T. O., Ayodele, E. G., & Dodo, J. D. (2009). A comparison of methods of computing geodetic coordinates from Cartesian coordinates. *National Journal of Space Research, 6*, 1–20.

[10] Jekeli, C., & Kwon, J. H. (2002). Geoid profile determination by direct integration of GPS inertial navigation system vector gravimetry. *Journal of Geophysical Research: Solid Earth, 107*(B10), 2217. https://doi.org/10.1029/2001JB001626.

[11] Mustafin, M., & Moussa, H. (2024). Accurate height determination in uneven terrains with integration of GNSS technology and geometric levelling: A case study in Lebanon. *Computation, 12*(3), 58. https://doi.org/10.3390/computation12030058.

[12] Odera, P. A., Musyoka, S. M., & Gachari, M. K. (2014). Practical application of the geometric geoid for heighting over Nairobi County and its environs. *Journal of Agriculture, Science and Technology, 16*(2), 176–186.

[13] Pebesma, E., & Graeler, B. (2022). *gstat: Spatial and spatio-temporal geostatistical modelling*. In Chapter 14: Kriging of *Spatial Statistics for Data Science: Theory and Practice with R*. Retrieved from https://www.paulamoraga.com/book-spatial/kriging.html.

[14] Prijatna, K., Lestari, R., Bramanto, B., Pahlevi, A. M., & Wijaya, D. D. (2024). Assessing the impact of methodological differences on geoid model performance. *Geographia Technica, 19*(2), 96–112. http://technicalgeography.org/pdf/2_2024/10_prijatna.pdf. https://doi.org/10.21163/GT_2024.192.10

[15] Suara, G., & Idowu, T. O. (2019). Optimum techniques for the conversion of space rectangular and curvilinear coordinates. *European Journal of Engineering and Technology Research, 4*(10), 147–151. https://doi.org/10.24018/ejeng.2019.4.10.1588.

[16] Suara, G. (2022). *Determination of geoidal undulation of points within the Federal University of Technology, Akure, Ondo State, Nigeria* (Unpublished Surveyors' Registration folio project). Surveyors Council of Nigeria.

[17] Suara, G., & Idowu, T. O. (2026). Development of a standalone computational tool for the conversion of space rectangular and curvilinear coordinates. *Nova Geodesia, 6*(1), 521.

[18] Tang, W., Wang, Y., Zou, X., Li, Y., Deng, C., & Cui, J. (2021). Visualization of GNSS multipath effects and its potential application in IGS data processing. *Journal of Geodesy, 95*, Article 103. https://doi.org/10.1007/s00190-021-01559-9.

[19] UN-GGCE (United Nations Global Geodetic Centre of Excellence). (n.d.). *Height datums and geoid models* (Workshop notes). https://ggim.un.org/UNGGCE/documents/CDWA/1/3_2_1%20-%20Height%20datums%20and%20geoid%20models.pdf (accessed March 10, 2026).